

Effect of channel doping on the low-frequency noise in GaN/AlGaN heterostructure field-effect transistors

A. Balandin,^{a)} S. Morozov,^{b)} G. Wijeratne, S. J. Cai, R. Li, J. Li, K. L. Wang,
and C. R. Viswanathan

Electrical Engineering Department, University of California—Los Angeles, Los Angeles, California 90095

Yu. Dubrovskii

Institute of Microelectronic Technology, Russian Academy of Sciences, Chernogolovka, 142432 Russia

(Received 13 April 1999; accepted for publication 9 August 1999)

We examined low-frequency noise in doped and undoped channel GaN/AlGaN/SiC heterostructure field-effect transistors with different Al content in the barrier. The observed noise spectra follow the $1/f^\gamma$ law with $0.8 \leq \gamma \leq 1.2$ for frequencies f up to 100 kHz. Our results indicate two orders of magnitude reduction in the input-referred noise spectral density in the undoped channel devices with respect to the noise density in the doped channel devices of comparable electric characteristics. Low temperature measurements reveal generation—recombination-type peaks in the spectra of the doped channel devices. Effects of the piezoelectric charges at the GaN/AlGaN interface are also discussed.

© 1999 American Institute of Physics. [S0003-6951(99)00740-8]

Advances in GaN-related compound materials and heterojunction field-effect transistors (HFET) have led to demonstration of high power density microwave operation of these devices.¹ Effective performance of the GaN high electron mobility transistors exhibiting the cutoff frequency f_T of 60 GHz and the maximum frequency f_{\max} exceeding 100 GHz has been recently reported by this group² and others. We have also shown that GaN HFETs grown on sapphire can operate with small low-frequency noise levels required for the microwave applications.³ The Hooge parameter extracted for these devices was on the order of $\alpha_H \approx 10^{-5} - 10^{-4}$ which is comparable to the noise level in commercial GaAs devices.

However, little is known about the physical origin of the low-frequency noise in GaN HFETs and the effect of the material quality on the noise level. The reported values of the Hooge parameter varies as much as four orders of magnitude.⁴⁻⁶ It is also not clear what model (the mobility fluctuation or the number fluctuation through random carrier trapping-detrapping) describes the best the $1/f^\gamma$ noise in the GaN system (γ being a parameter close to 1). The question of particular importance for the GaN system, related to the physical origin of the noise, is how the channel doping influences the low-frequency noise. It has been previously shown that the nitrides have large piezoelectric coefficients which lead to strong electric polarization on (0001) faces of the wurtzite structures typically used for GaN HFETs.⁷ The latter results in appreciable charge densities which are large enough (on the order of $10^{12} - 10^{13} \text{ cm}^{-2}$) to design HFETs without any channel or barrier doping.⁸

In this letter we report low-frequency noise measurements of the doped and undoped channel GaN/AlGaN HFETs grown on semi-insulating 4H-SiC substrates. The

layered structures of the devices of both types are shown in Fig. 1(a). The actual aluminum content was determined by photoluminescence (PL) and Rutherford backscattering (RBS) and found to be 14% for the doped channel device ($P1$), and 33% for the undoped channel device ($F2$). The piezoelectric effect, barrier, and channel doping resulted in a sheet carrier concentration $\sigma_s(T=300 \text{ K}) = 1.1 \times 10^{13} \text{ cm}^{-2}$, $\sigma_s(T=77 \text{ K}) = 8.6 \times 10^{12} \text{ cm}^{-2}$ for $P1$; and $\sigma_s(T=300 \text{ K}) = 1.2 \times 10^{13} \text{ cm}^{-2}$, $\sigma_s(T=77 \text{ K}) = 1.2 \times 10^{13} \text{ cm}^{-2}$ for $F2$. Electron Hall mobility at 300 K was determined to be $616 \text{ cm}^2/\text{V s}$ for doped HFETs, and $1339 \text{ cm}^2/\text{V s}$ for undoped HFETs. At 77 K the mobilities are 1037 and $5365 \text{ cm}^2/\text{V s}$, respectively. The dc current-voltage characteristics in the range of the drain and gate voltages used for the noise measurements are shown in Fig. 1(b).

It is interesting to note that at room temperature the total sheet carrier concentrations are about the same for both $P1$ and $F2$ HFETs. The piezoelectric charge density in an AlGaIn/GaN heterostructure is proportional to the aluminum mole fraction.⁸ Thus, the higher Al content of the barrier layer of the undoped channel device approximately compensates the absence of the channel doping. Indeed, σ_s due to the channel doping and piezoelectric effect can be written approximately as $\sigma_s = \sigma_p + N_d W$, where σ_p is the surface density of piezoelectrically induced charges, N_d is the volume doping concentration, and W is the channel layer thickness. Knowing the resulting sheet electron concentration, we can express the difference in the piezoelectrically induced charges as $\Delta\sigma_p \equiv \sigma_p^u - \sigma_p^d = \sigma_s^u - \sigma_s^d + N_d W$, where superscripts u and d denote undoped and doped channels, respectively. Substituting the appropriate numbers in the above equation, we finally obtain $\Delta\sigma_p = 1.1 \times 10^{13} \text{ cm}^{-2}$. According to Ref. 8, σ_p rises approximately linearly with the Al mole fraction x_{Al} , following the rule $\Delta\sigma_p/\Delta x_{\text{Al}} = 5 \times 10^{13} \text{ cm}^{-2}$. Applied to our devices, this gives the change in the piezoelectric charge density of about $0.95 \times 10^{13} \text{ cm}^{-2}$. As one can see, this number is very close to $\Delta\sigma_d$ obtained from the actual sheet carrier densities (within 14% error).

^{a)}Present address: Department of Electrical Engineering, University of California, Riverside, CA 92521; electronic mail: alexb@ee.ucla.edu

^{b)}On leave from the Institute of Microelectronic Technology, Russian Academy of Sciences, Chernogolovka, Russia.

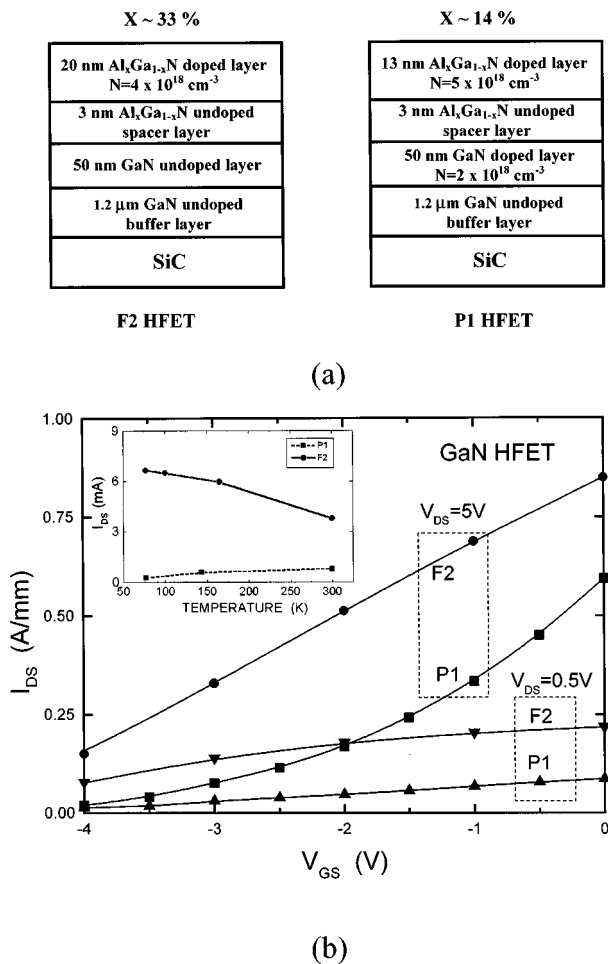


FIG. 1. (a) Uncapped layered structure of the undoped channel (*F2*), and the doped channel (*P1*) GaN HFETs. Note that *F2* HFET has a higher Al content in the barrier layer and, thus, a higher piezoelectric charge density to compensate for the absence of channel doping. (b) The dc current-voltage characteristics for *P1* and *F2* GaN HFETs shown for the same range of the drain and gate biases used in the noise measurements. Inset shows drain current as a function of temperature for both devices biased at $V_{DS} = 0.5 \text{ V}$ and $V_{GS} = -1.0 \text{ V}$.

This confirms the fact that piezoelectric charge approximately compensates the absence of the channel doping and makes the comparative noise study meaningful.

The devices selected for this study have a fixed gate length $L_G = 1.0 \mu\text{m}$ and a gate width $W = 50 \mu\text{m}$. At drain-source voltage $V_{DS} = 5 \text{ V}$, a doped channel device *P1* has the transconductance $g_m = 160 \text{ mS/mm}$ at $V_{GS} = 0 \text{ V}$; an undoped channel device *F2* has the transconductance $g_m = 182 \text{ mS/mm}$ at $V_{GS} = -2.5 \text{ V}$. The measurements are carried out for both the linear region of the device operation corresponding to low V_{DS} , and for the onset of the saturation region of operation (subsaturation). The experimental setup used for these measurements is similar to the one described in Ref. 6.

Experimental noise spectra of two types of GaN HFETs for fixed drain voltages and different gate biases are shown in Fig. 2. The threshold voltages are about $V_T = -4.5 \text{ V}$ and $V_T = -5.5 \text{ V}$ for *P1* and *F2*, respectively. As seen in Fig. 2, for all values of the gate bias in the linear regime ($V_{DS} = 0.5 \text{ V}$), the input-referred noise spectral density is about *two orders of magnitude lower* for the undoped channel device than that for the doped channel device. The difference in

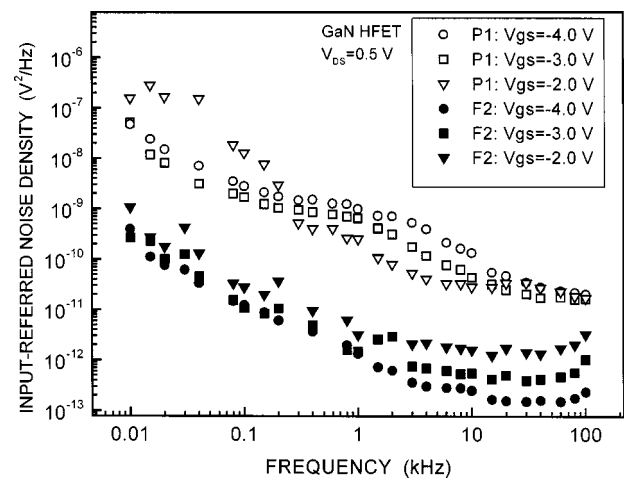


FIG. 2. Input-referred noise spectra for the doped channel GaN HFET (*P1*) and the undoped channel GaN HFET (*F2*) in the linear regime ($V_{DS} = 0.5 \text{ V}$). Note a significant difference (up to two orders of magnitude) in the input-referred spectral density between two types of the devices for all gate biases.

the low-frequency noise level is particularly significant in view of the fact that these devices have comparable characteristics, e.g., total sheet carrier concentration, g_m , and V_T . Figure 2 also shows a trace of the g - r bulge in the noise spectra of the doped channel devices. The slope γ of the $1/f^\gamma$ dependence is in the range $0.8 \leq \gamma \leq 1.2$. A noticeable deviation of γ from unity may be due to carrier trapping-detraping mechanism of the low-frequency noise.⁹ Although not shown in the picture, in the subsaturation region of operation ($V_{DS} = 5 \text{ V}$), the noise spectral density for the undoped channel device is again significantly smaller than that for the doped channel device.

In order to have a quantitative assessment of the overall noise in the device, we extract the Hooge parameter α_H using the regular equation

$$\alpha_H = \frac{S_V}{V^2} N f, \quad (1)$$

where f is the frequency, N is the total number of carriers under the gate calculated from the drain-source current at which the noise was measured, and S_V is the input-referred noise spectral density. The calculation procedure is similar to that reported in Refs. 5 and 6. The significant difference in the noise spectral densities, as well as the mobility difference between the doped and undoped channel devices, translates into a corresponding difference in the Hooge parameters, particularly in the linear regime ($V_{DS} = 0.5 \text{ V}$). At $V_{GS} = -2 \text{ V}$ the Hooge parameters are $\alpha_H^{\text{doped}} = 8.3 \times 10^{-3}$ and $\alpha_H^{\text{undoped}} = 7.8 \times 10^{-5}$. In the subsaturation region the difference is less pronounced, although channel doping still degrades the noise figure: $\alpha_H^{\text{doped}} = 7.8 \times 10^{-3}$ and $\alpha_H^{\text{undoped}} = 1.3 \times 10^{-3}$ for $V_{GS} = -4 \text{ V}$ and $V_{DS} = 5 \text{ V}$, respectively.

The low temperature noise characteristics of doped channel devices were also examined. Figure 3 shows these characteristics in the subsaturation region of the device operation. A pronounced peak is observed at about 3–4 kHz for the doped channel (*P1*) devices. At the same time, no peaks in spectra of the undoped channel device were observed. The spectrum of the *F2* GaN HFET has a corner frequency of

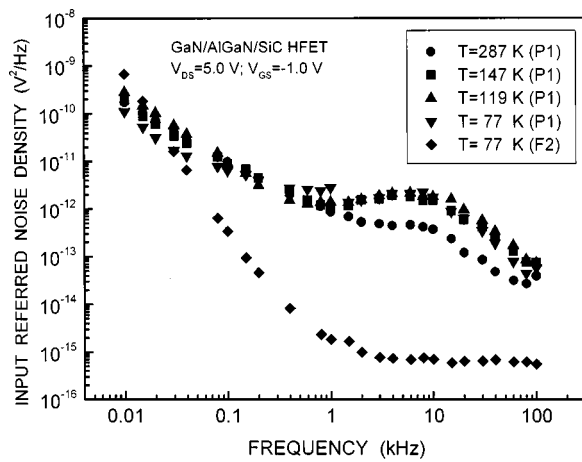


FIG. 3. Low temperature noise characteristics of the GaN HFETs in the subsaturation regime. Generation-recombination ($g-r$) bulges are clearly seen in spectra of the doped channel device ($P1$) at frequency $f \approx 3-4$ kHz. There are no traces of $g-r$ bulges in the spectra of the undoped channel ($F2$) device (shown at 77 K).

about 1 kHz determined by the Johnson noise. The level of Johnson noise $6 \times 10^{-16} \text{ V}^2/\text{Hz}$ is in agreement with the Nyquist formula.

The Lorentzian shape and the position of the peaks in $P1$ device spectra seems to suggest its generation-recombination origin ($g-r$). This peak may be an indication that carrier number fluctuation via trapping is the dominant noise mechanism in the doped GaN systems. Fitting the peaks by the method outlined in Ref. 10, we were able to determine that the activation energy is about 0.35 eV.

In conclusion, we examined low-frequency noise in doped and undoped channel GaN/AlGaIn/SiC HFETs. A higher aluminum content of the undoped channel devices leads to a higher piezoelectrically induced charge density, thus making up for the absence of doping and allowing for a

meaningful comparison of the noise levels for both types of the devices. Our results reveal a two-orders-of-magnitude reduction in the input-referred noise spectral density of the undoped channel device with respect to the noise density of the doped channel devices with comparable electric characteristics. This difference in the noise level can be attributed to the different nature of carriers in the channels of HFETs (piezo-induced carriers in the $F2$ device versus carriers due to external doping in the $P1$ device) and corresponding difference in carrier fluctuation and scattering processes. The low temperature noise spectra for doped devices shows clear $g-r$ peaks. The latter may shed new light on the physical origin of low-frequency noise in GaN structures.

This work was supported in part by the DoD MURI-ARO program on "Low-Power/Low-Noise Electronic Technology for Mobile Communications" (Dr. James Harvey).

- ¹G. J. Sullivan, M. Y. Chen, J. A. Higgins, J. W. Yang, Q. Chen, R. L. Pierson, and B. T. McDermott, *IEEE Electron Device Lett.* **19**, 198 (1998).
- ²S. J. Cai, R. Li, Y. L. Chen, L. Wong, W. G. Wu, S. G. Thomas, and K. L. Wang, *Electron. Lett.* **34**, 2354 (1998).
- ³A. Balandin, S. Cai, R. Li, K. L. Wang, V. Ramgopal Rao, and C. R. Viswanathan, *IEEE Electron Device Lett.* **19**, 475 (1998).
- ⁴M. E. Levinshtein, F. Pascal, S. Contreras, W. Knap, S. L. Rumyantsev, R. Gaska, J. W. Yang, and M. S. Shur, *Appl. Phys. Lett.* **72**, 3053 (1998); M. E. Levinshtein, S. L. Rumyantsev, R. Gaska, J. W. Yang, and M. S. Shur, *ibid.* **73**, 1089 (1998).
- ⁵D. V. Kuksenkov, H. Temkin, R. Gaska, and J. W. Yang, *IEEE Electron Device Lett.* **19**, 222 (1998).
- ⁶A. Balandin, S. Morozov, S. Cai, R. Li, K. L. Wang, G. Wijeratne, and C. R. Viswanathan, *IEEE Trans. Microwave Theory Tech.* (Special issue on technologies for mobile wireless communications) **47**, 1413 (1999).
- ⁷A. Bykhovski, B. Gelmont, and M. Shur, *J. Appl. Phys.* **74**, 6734 (1993).
- ⁸P. M. Asbeck, E. T. Yu, S. S. Lau, G. J. Sullivan, J. Van Hove, and J. Redwing, *Electron. Lett.* **33**, 1230 (1997).
- ⁹Z. Celik-Butler and T. Y. Hsiang, *Solid-State Electron.* **30**, 419 (1987).
- ¹⁰J. R. Kirtley, T. N. Theis, P. M. Mooney, and S. L. Wright, *J. Appl. Phys.* **63**, 1541 (1988).